Chapter 5

Reaction of atomic oxygen with the D-covered Si(100) surfaces

So far, in the previous chapters, I experimentally studied the feature of D abstraction by H on the D/Si surfaces. It was clearly shown that H atoms can directly abstract D adatoms to form HD molecules as well as indirectly to generate D_2 desorptions. Such adatom abstractions by H atoms may be also possible for O atoms as I reviewed in the Introduction. Some similarities can be found between the H- and O-induced abstraction reactions. Shimokawa et al.[1] and Rahman et al.[2] studied D abstraction by O on Si(100) and Si(111) surfaces and found that both D_2 and D_2O molecules were desorbed as O atoms impinge on the D/Si(100)[1] and D/Si(111)[2]. The O-induced D_2 desorptions exhibit a clear peaking at around 640 K in the D_2 yield versus *T*s curve likely to the H-induced D_2 desorptions, suggesting dideuterides are responsible for the D_2 desorption reaction. Moreover, the O-induced D_2 desorption exhibited an induction time to reach the maximum rate. Adsorption of O atoms onto D/Si(100) could form locally high density of dideuterided area after rearranging the D adsorption sites. O adsorption in between two Si atoms must be highly exothermic reaction.[3] Therefore, local heating could induce recombinative desorption either via β_1 channel from monohydride phase or via β_2 channel from dihydride phase. However, Rahman et al.[2] did not check whether dideuterides can enhance D_2 desorption or not. On the other hand, rates of D_2O desorptions jump up immediately when the O exposure started. Hence, they considered that this rapid rate jump due to either a simultaneous pick up of two D atoms by O atoms or a sequential two steps abstraction. If they did the same experiment on the surfaces saturated with dideuterides, they could establish which mechanism was operative.

In this chapter, I investigate the kinetic mechanisms of O-induced D_2 and D_2O desorptions by testing the reactions on the Si(100) surfaces which are terminated with

only monodeuterides or with mixture of monodeuterides and dideuterides. Thereby possible role of dideuterides to the O-induced D_2 and D_2O desorptions is clarified. Not only the continuous O beam but also pulsed O beam is used to reveal whether the two desorption reactions include fast or slow desorption channels.

5.1 Experiment

Since most common experimental parts were described in Chapter 2, here only specific related parts are explained. The fluxes of D atoms at the surface were evaluated to be about $7x10^{12}$ $cm^{-2}s^{-1}$ and $1x10^{13}$ $cm^{-2}s^{-1}$ for O atoms.[1] A continuous O-beam was modulated by a rotating chopper of 0.1 Hz. Two types of pulsed O-beams were generated by two choppers having slots of 50% and 5% duty ratio, producing the pulsed O-beam with 5 s on- and 5 s off-cycles and 0.5 s on- and 9.5 s off-cycles, respectively (Fig. 2.5). The measured D_2O rate curves, detected by the QMS, had a background effect, which was brought by the O-beam from the beam chamber into the reaction chamber. They could be produced somewhere in the O-beam chamber via possible reaction between O and D atoms on the chamber wall. Such D_2O background was subtracted from the raw rate curves. The D-covered surfaces were prepared by exposing the clean Si(100) surface to D atoms at various surface temperatures. Monodeuteride surfaces were prepared by D dosing at 573 K where dideuterides are not allowed because of β_2 TD. The initial D coverage, θ°_D, was changed by controlling D dosing time. On the other hand, dideuteride rich surfaces were prepared by sufficient D-dosing at given temperatures below 500 K. The initial coverage of surface dideuterides depended on the dosing temperature: for example, 0.5 ML (θ°_D=1.5 ML) at 300 K, 0.33 ML (θ°_D=1.33 ML) at 443 K, and 0 ML (θ°_D=1.0 ML) at 573 K.

5.2 D/Si(100) surfaces exposed to O beam.

The D/Si(100) surface was exposed to the continuous and pulsed O-beam on various initial D coverages (θ°_{D}) at various surface temperatures (*T*s). Desorbed D_2 and D_2O molecules were detected with the QMS in angle integrated mode during the surface exposure to O-beam.

5.2.1 Direct O beam effect

Figures 5.1 and 5.2 show plots of D_2 and D_2O rate curves measured when continuous O-beam was admitted on the saturated and monolayer (ML) surfaces as a function of O-exposure time, t. It should be mentioned here that saturated and monolayer surface corresponded to dideuteride rich and dideuteride free surfaces, respectively. It is quite obvious that maximum D_2 rate on the monodeuteride/dideuteride surfaces at 300K is nearly six times larger than that on the monodeuteride surface. With increasing *T*s, this behavior diminished due to decrease of surface dideuterides. This nonlinear increase in the D_2 rate with increasing dideuteride coverage suggests that dideuterides play a decisive role in the O-induced D_2 desorption. On the other hand, one may notice in Fig. 5.2 that the dideuterides enhance D_2O rate only slightly super linearly at *T*s=300 K and at higher *T*s, this effect is negligible. Both D_2 and D_2O rate curves plotted in Figs. 5.1 and 5.2 exhibit a feature that their initial rate jumps up quickly following the incident O-beam. The maximum D_2 rates showed a time lag from the beginning of the O-beam, but the D_2O rate curves did not show such a time lag. Both of the rate curves decreased almost exponentially with time t, after these peaks. These decrease in the desorption rates are merely due to consumption of abstractable D adatoms. However, as we noted in the D_2 TD spectra after the O exposure,[1] the D

adatoms still remained on the surface even when the rates of D_2O or D_2 desorptions became nearly zero. This fact suggests that once a certain amount of O atoms are adsorbed, Si–D bonds become stronger. Indeed, based on ab initio calculation, it is reported that Si–H bond energy has been stabilized by backbonding oxygen atoms,[4] which was experimentally supported in the Si–H vibrational spectra[5,6] and the D_2 thermal desorption spectra.[7]

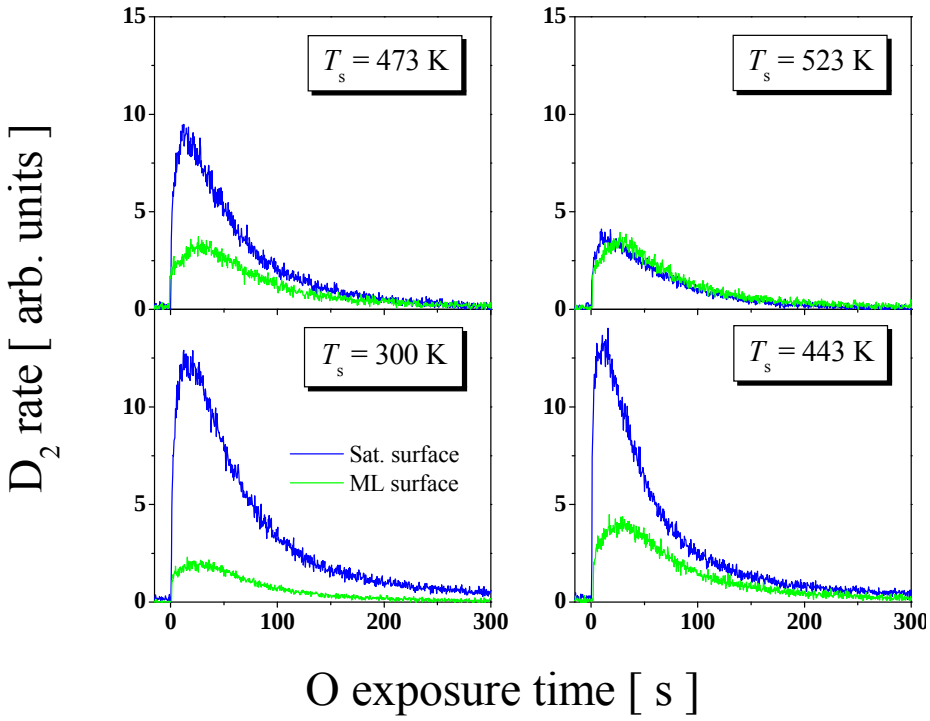

Fig. 5.1 Plots of O-induced D_2 rate data as a function of continuous O-beam exposure time at different surface temperature (*T*s) on D saturated and monolayer surfaces.

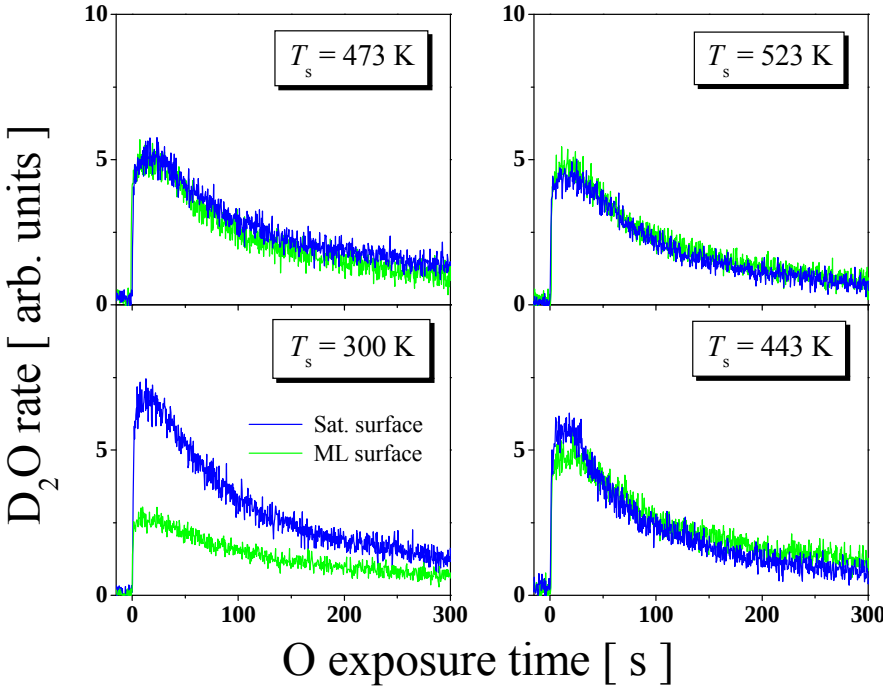

Fig. 5.2 Plots of O-induced D_2O rate data as a function of continuous O-beam exposure time at different surface temperature (*T*s) on D saturated and monolayer surfaces.

5.2.2 Pulsed O beam effect

In order to know more clearly how quickly the O-induced desorption reactions respond to the incident O atoms, we measured D_2 and D_2O rate curves employing the pulsed O-beam. Fig. 5.3 shows D_2 (left panel) and D_2O (right panel) desorption rate curves obtained when the pulsed O-beam with 5 s on- and 5 s off-cycles were admitted at various *T*s to the monodeuteride/dideuteride surfaces. The insets show the expanded time profiles for first few cycles. Both the D_2 and D_2O desorption rates sharply increase at on-cycles and rapidly decrease at off-cycles. This quick response to the pulsed O-beam suggests that the D_2 and D_2O desorptions are prompt in nature. However, as shown in Fig. 5.3 the measured desorption rates do not turn into zero even at O-beam off-cycles. This nonzero desorption rate at off-cycles suggests that some delayed desorption could be involved in the process. This may be true for the D_2 molecules, but

not for the D_2O molecules. The reason is that the desorbed D_2O molecules could adsorb onto the chamber wall and then desorb again into the background circumstance, giving rise to the D_2O intensity at off-cycles. In contrast, D_2 molecules may not adsorb onto the chamber wall and therefore the observed D_2 intensity at off-cycles could be ascribed to be a delayed desorption from the Si(100) surfaces.

The shorter pulses of the O-beam having 0.5 s on- and 9.5 s off-cycles revealed a somewhat interesting feature in the delayed desorption. Fig. 5.4 shows three rate curves which were obtained by collecting QMS signals for 20 pulses, (a) at the very early stages of the pulsed O-beam exposure on the monodeuteride/dideuteride surfaces, (b) same as for (a) but on the 1 ML monodeuteride surfaces, and (c) same as for (b) but after 7 minutes of O-exposure. The insets to Fig. 5.4 a–c show the expanded time profiles of the trailing edges of the pulsed D_2 rate curves. Because of the tail in the rate curve plotted in (a) the delayed desorption is obvious for the monodeuteride/dideuteride surface, more simply, due to presence of dideuterides. On the other hand, no tail in the

curve (b) suggests no occurrence of such delayed desorption on the monodeuteride surface, due to absence of dideuterides. However, as shown in (c), a tail can be recognized even on the initially prepared monodeuteride surface after the adsorption of certain amount of O atoms. If delayed desorption takes place only on dideuterides rich surfaces as found in (a), the tail appeared in the rate curve in (c) would suggest that the O adsorption locally pile up dideuterides onto the initially prepared monolayer (1 ML) D-covered Si(100) surfaces. The time lag of the D_2 rate curves in Fig. 5.3 (left panel) could also be caused by such dideuterides excessively piled on the surfaces during O exposure. The presence of such excess dideuterides may be further supported by the

experimental observation that if the Si(100) surface contains 0.1 ML O adatoms, the β_2 TD peak appears even at as low as 0.5 ML D coverage.[7]

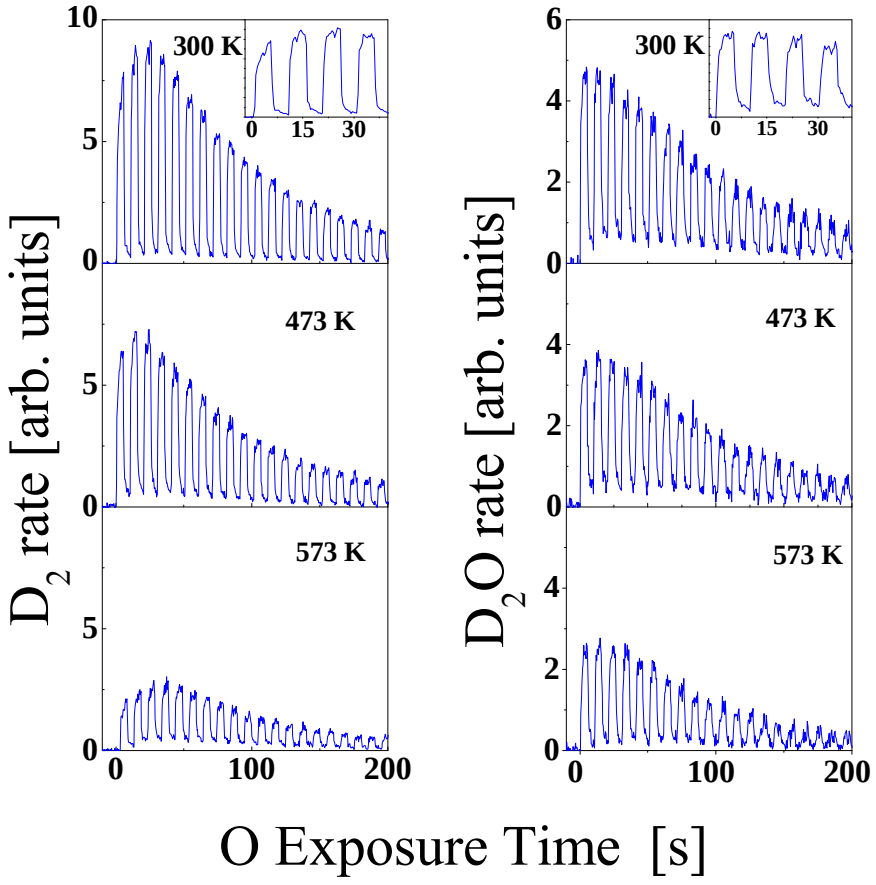

Fig. 5.3 Plots of O-induced D_2 (left) and D_2O (right) rate curves as a function of pulsed O-beam (5 s on- and off-cycles) exposure time at various surface temperature (*T*s) on D saturated (dideuteride rich) surfaces. The insets show the rate curves expanded in the time domain for the first few cycles of the pulsed desorption events.

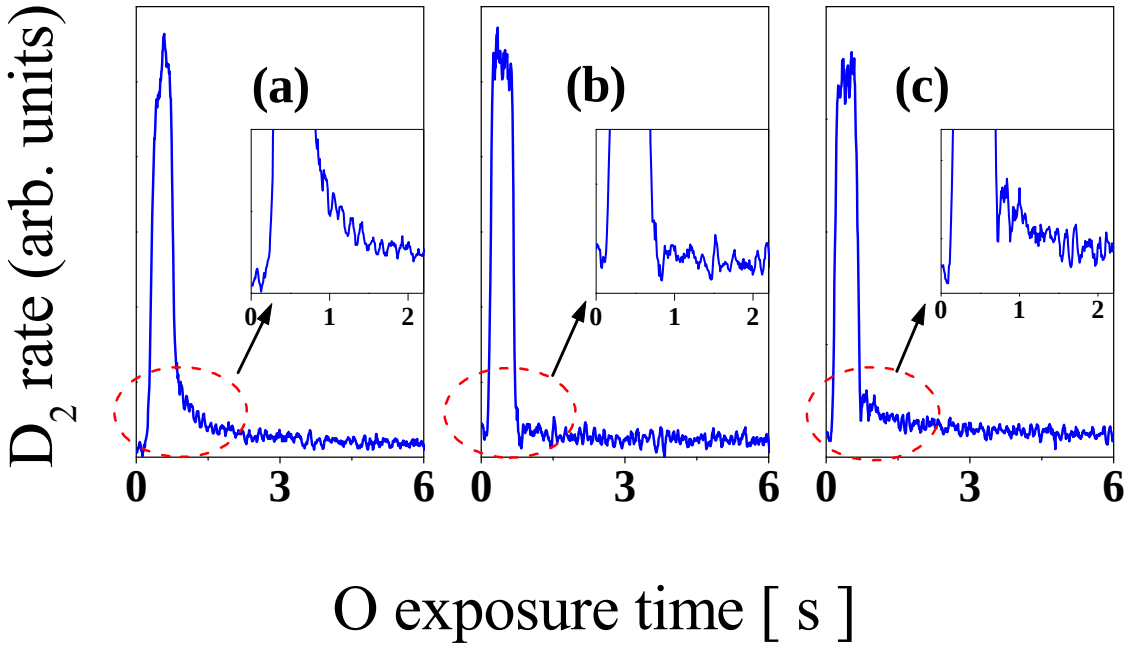

Fig. 5.4 Plots of D_2 rate curves obtained at 300 K with the short pulsed O-beam consisting of 0.5 s on- and 9.5 s off-cycles. The curve in (a) for θ°_{D} = 1.5 ML and the curve in (b) for θ°_{D}=1.0 ML were accumulated for the first 20 pulses on the Si(100) surfaces. The rate curve in (c) was obtained by accumulating 20 pulses after 7 min O-beam exposure when the D_2 rate reached nearly maximum. The insets show the time profiles expanded for the trailing edge of the rate curves, confirming the delayed desorption more clearly.

5.3 Temperature dependence

The maximum D_2 rates measured on the D/Si(100) surfaces were plotted as a function of *T*s in Fig. 5.5, where the curves (a) and (b) were obtained on the surfaces saturated with dideuterides at given *T*s and on the surface covered with 1 ML monodeuterides, respectively. It is obviously seen that D_2 rates are much larger on the monodeuteride/dideuteride surfaces (curve-a) than on the monodeuteride surfaces (curve-b). This difference becomes prominent at lower temperatures, where dideuterides coverages were higher. The D_2 rates measured on the monodeuteride/dideuteride surface decrease quite rapidly with increasing *T*s around 500 K, while the rates

measured on the monodeuteride surfaces tend to mildly increase with *T*s. The decrease of D_2 rate with *T*s in the former case is merely due to the decrease of the initially prepared dideuteride coverages with increasing D-dosing temperatures. D_2 desorptions can be also induced by H atoms on the D/Si(100) surfaces. As was reviewed in introduction, the dideuterides on the surface also play a decisive role for the H-induced D_2 desorption.[8] However, the *T*s dependence of D_2 rates is clearly different between the O- and H-induced processes. As shown in curve (c) of Fig. 5.5, the rate of H-induced D_2 desorption increases with increasing *T*s.[9] Thus the trend of the O-induced desorption is quite opposite to that of the H-induced desorption; suggesting the mechanism of the O-induced D_2 desorption differs from that of the H-induced one. In Fig. 5.6, I plot D_2O rate curves as a function of *T*s on the Si(100) surfaces saturated with dideuterides at given *T*s (curve-a) and θ°_{D} = 1.0 ML (curve-b). The *T*s dependence of D_2O rate appears similarly to that of D_2 rates as plotted in Fig. 5.5 for the surface saturated with dideuterides at *T*s. The measured D_2O rates are larger on the monodeuteride/dideuteride surface than on the monodeuteride one. Taking the data obtained at 423 K, for instance, the D_2O rates measured on the surfaces containing 0.33 ML dideuterides are nearly 1.5 times the rate measured on the monodeuteride surface. However, one should remind that the size of net increase in the D_2O rate is much smaller than that for D_2 rate. This fact suggests that the D_2O desorption is less affected by dideuterides, compared with the D_2 desorption.

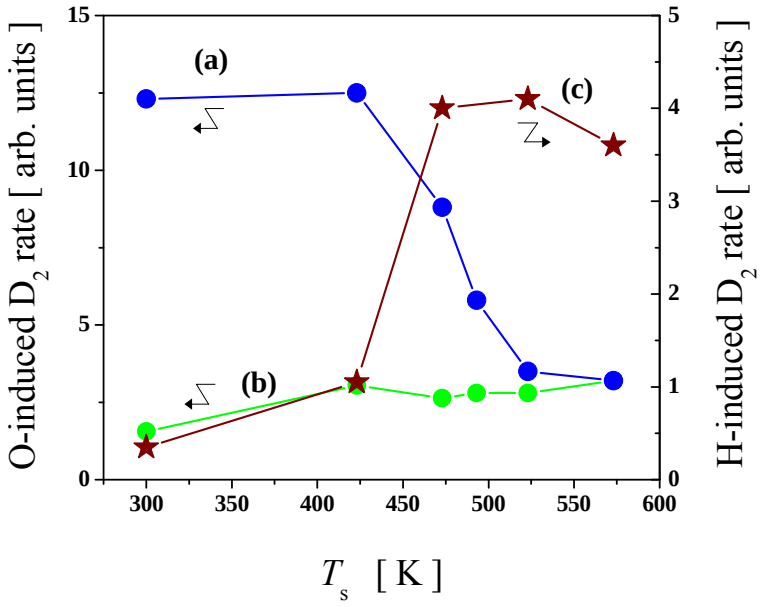

Fig. 5.5 Plots of the initial D_2 rate steps as a function of *T*s. (a) The surfaces were prepared after sufficient D dosing at given Ts, i.e., $\theta^{\circ}_{D} \geq 1.0$ ML. (b) $\theta^{\circ}_{D} = 1.0$ ML. For comparison, H-induced D_2 rate steps were also plotted in curve (c). The data of the curve (c) were obtained from Ref. 9.

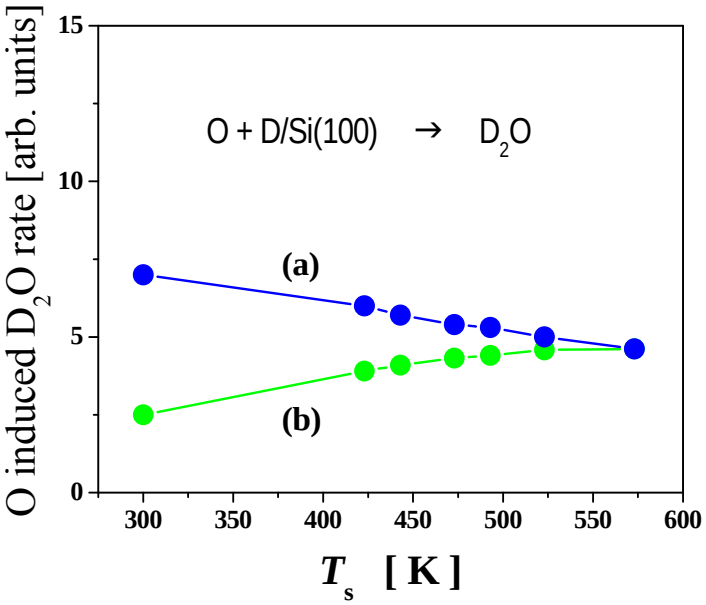

Fig. 5.6 Plots of D_2O rate steps as a function of *T*s on the D saturated coverage (rich in dideuteride) prepared at given *T*s (curve-a) and on the monodeuteride surface with $\theta^{\circ}_{D} = 1.0$ ML (curve-b).

5.4 Activation energies and reaction mechanisms

5.4.1 O induced D_2 desorption

In order to understand kinetic mechanism of the O-induced desorption of D_2 and D_2O molecules from the D/Si(100) surfaces, desorption orders of the two reactions should be evaluated. Desorption order, m, of D_2 or D_2O molecules may be defined by the desorption rate equation, $R \propto \theta_D^m$, where R is the desorption rate. To evaluate reaction order, m, D_2 and D_2O rate curves were measured at 443 K for various θ°_D. The size of the initial rate steps can be a measure from the nascent desorption rate on the O-free surfaces. We make a log–log plot of initial D_2 rates as a function of θ°_D in Fig. 5.7. One can notice that desorption is categorized into either a low coverage regime or a high coverage one. The two regimes are discriminated by the kink recognized around 1.0 ML. The slope of the curve is evaluated to be 1.8 ± 0.1 and 3.5 ± 0.2 for the D_2 desorption along the low and high coverage regime, respectively. Hence, it may be understood that the D_2 desorption is governed by the second-order rate law in θ°_D on the monodeuteride surfaces, and is governed by the 3.5th-order rate law on the monodeuteride/dideuteride surfaces. The second-order rate law found in the D_2 desorption suggests that two recombining D atoms have not been prepared like occupied Si dimer or DSi–SiD but two recombining D adatoms are chosen spatially randomly. To explain the observed second-order D_2 desorption reasonably, we invoke a hot-atom/hot-complex mediated mechanism. According to this mechanism, an incident O atom kicks out a D atom into an energetically excited state, denoted as D*. After that, it is immediately trapped in a cell of nearby dimer either in the neighboring or in the same Si dimer row, forming a hot complex (D + DSi–SiD)*. During the energy relaxation of the hot complex, the hot D atom can abstract one of the two D adatoms

bonded to the Si dimer. Thus, one molecule of D_2 is desorbed due to incidence of one O atom from the D/Si(100) surface. This is the extended version of the hot-complex mechanism, which was proposed by Hayakawa et al.[10] for the first time in the reaction system $H_{(g)} + D/Si(100)_{(s)} \rightarrow HD_{(g)}$. As was supposed in their studies, longly lived hot atoms are not allowed on the Si surfaces, but they are promptly converted to an immobile hot-complex. Thus, D*s generated by O atoms could be simply considered to act as if they were gas phase atoms incident to the sites for abstraction reaction. The hot-atom/hot-complex mediated mechanism is illustrated in Fig. 5.8. By this mechanism, each rate of the D* formation and the subsequent D abstraction from the hot complex may be proportional to θ°_{D}. Hence, the second-order rate law observed for the D_2 desorption may be explained along this picture. On the other hand, the nearly fourth-order D_2 desorption was found on the dideuteride rich (3x1) monodeuteride/dideuteride surfaces. Such a high reaction order could be related to the β_2 TD since it obeys the second-order rate law with respect to dideuteride coverage, i.e., four D atoms are involved in the reaction. The adsorption energy of O-insertion into Si back bonds is as high as 1 eV.[3] Such high adsorption energy could locally heat up the surface, making the (3x1) monodeuteride/dideuterides phase unstable towards molecular emission. Consequently, D_2 molecules could desorb from such locally heated surface via the β_2 TD channel even at temperatures lower than the typical β_2 TD. The measured desorption order is apparently fractional,~3.5th. This fractional order could be reconciled by including possible contribution by the above mentioned second order desorption. In this case, D*s ejected along the same Si dimer row may be trapped in a cell of the nearest neighbor DSi–SiD to make a hot-complex as a precursor of the subsequent D_2 desorption.

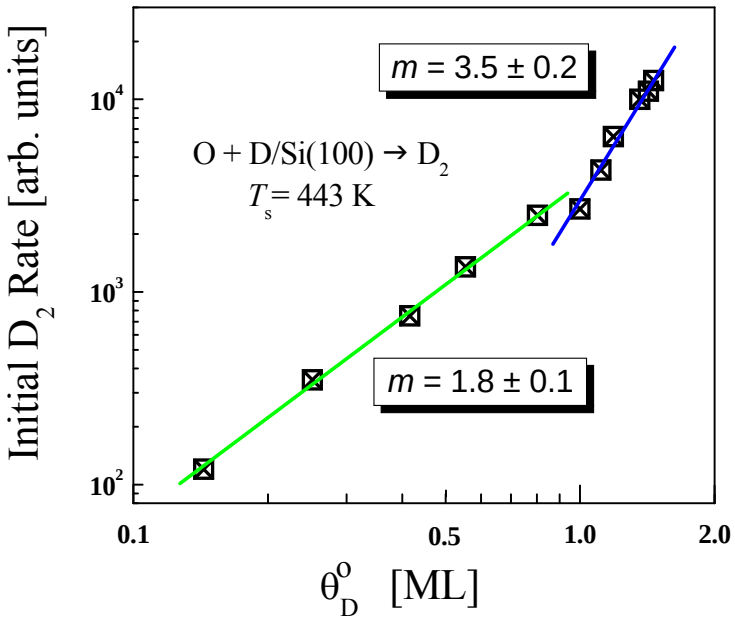

Fig. 5.7 Log–log plots of D_2 rate steps as a function of θ°_D at 443 K. The data can be fit with a D_2 rate equation, $R \propto \theta_D^{m}$, where R is the rate of D_2 desorption, m is the desorption reaction order. The best curve fit yields m = 1.8 ± 0.2 and 3.5 ± 0.1 for $\theta^{\circ}_D \leq 1.0$ ML and $\theta^{\circ}_D \geq 1{:}0$ ML, respectively. This result suggests that O-induced D_2 desorption on the monodeuteride surface is governed by a second-order rate law with respect to D coverage while on the monodeuteride/dideuteride surface it is governed by a 3.5th-order rate law.

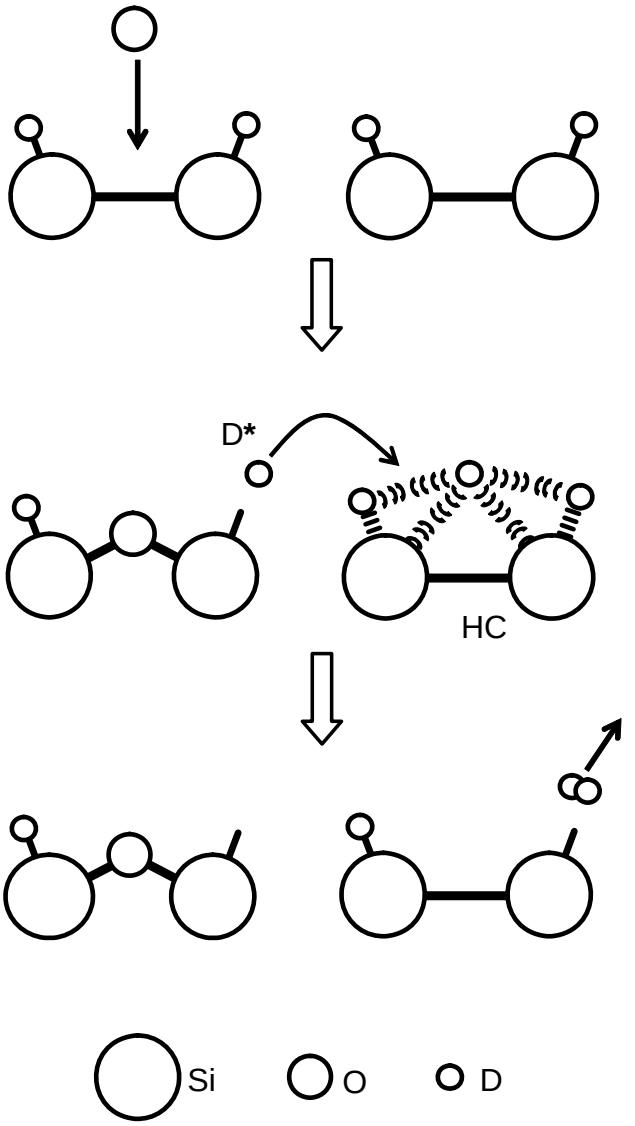

Fig. 5.8 Model of O-induced D_2 desorption from the monodeuteride surfaces. First stage: an O atom has been adsorbed at the Si–Si dimer bond to make oxygen bridging in between two Si atoms. The excess adsorption energy gained upon O adsorption causes emission of a hot D*. Second stage: the D* will be trapped in a chemisorption potential of a nearby DSi–SiD cell, forming a hot-complex (HC). Third stage: the hot D* in the HC proceeds associative desorption with one of the two D adatoms in DSi–SiD unit.

5.4.2 O induced D_2O desorption

In case of D_2O desorption, a nearly second-order desorption kinetics was found on both the monodeuteride/dideuteride and monodeuteride surfaces as shown in Fig. 5.9. This result seems to be natural since two D adatoms are picked up by an atom of O in the process. As shown in Fig. 5.3, the D_2O desorption reaction occurs quite promptly upon admission of the pulsed O-beam. Compared with the case of D_2 rate curves, which exhibited the induction time to reach the maximum rate, the measured D_2O rate curves do not show such a clear induction time as shown in Fig. 5.2. As discussed, the presence of the induction time for the D_2 rate curves may be due to D_2 desorption enhanced by dideuterides which are piled up during the O-beam exposure (Fig. 5.2). In contrast, no induction times were noticed in the D_2O rate curves may be understood in such a way that simultaneous abstraction of two D atoms by an O atom is not required to form a D_2O molecule. This can be further confirmed in Fig. 5.6 since the extent of increase in the D_2O rate with increasing θ°_{D} from 1.0 ML to 1.5 ML is milder than that of D_2 rate as plotted in Fig. 5.5. On the basis of these facts, in Fig. 5.10, we propose a two step desorption mechanism by which an incident O atom first picks up a D atom to form a hot OD* molecule which then abstract a nearby D adatom to generate D_2O desorption. This mechanism has been proposed by Rahman et al.[2] for the O-induced D_2O desorption on the Si(111) surface. Similar D_2O formation mechanism is also reported when D-covered Pt(111) surface was exposed to gaseous O atoms.[11] If OD*s fail to abstract a D adatom, they may stick to surface Si atoms as a relaxed Si–OD species. Recently, a vibrational peak attributable to Si–OH stretching mode was measured in an electron energy loss spectroscopy on the H/Si(100) surface after the surface exposure to O atoms.[12]

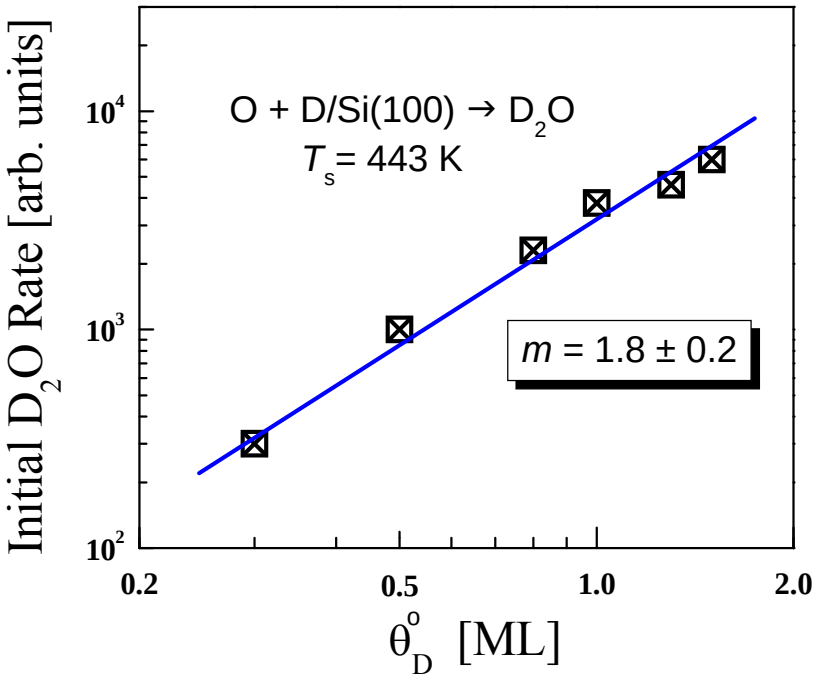

Fig. 5.9 Log–log plots of D_2O rate step as a function of θ°_{D} at 443 K. The data can be fit with a D_2O rate equation, $R \propto \theta_D^{m}$, where R is the rate of D_2O desorption, m is the desorption reaction order. The best curve fit yields m = 1.8 ± 0.2. This result suggests that the O-induced D_2O desorption on the monodeuteride surface is governed by a second-order rate law with respect to θ°_{D}.

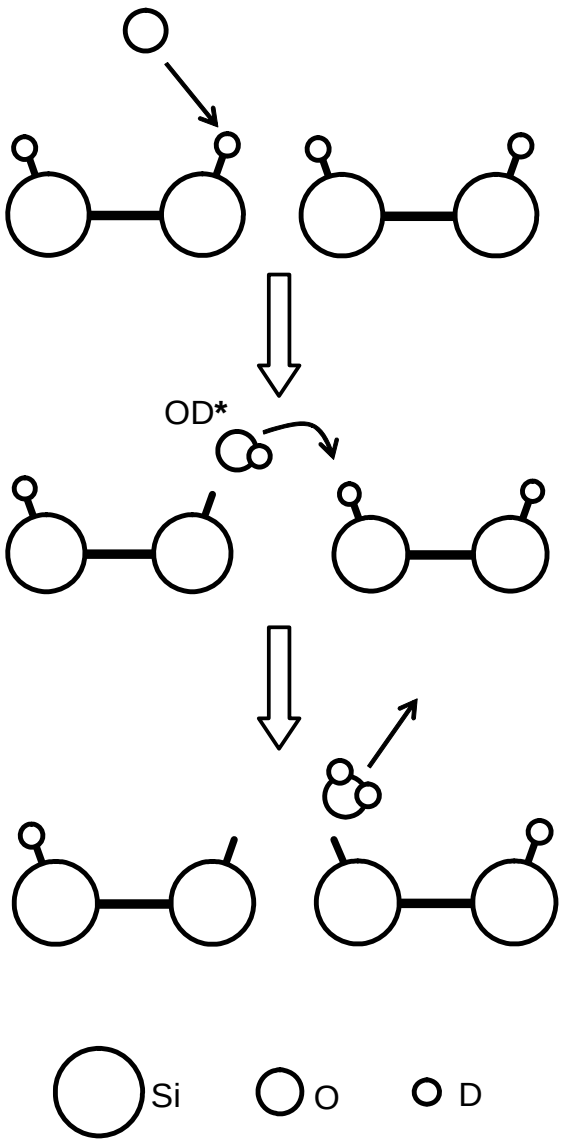

Fig. 5.10 Proposed model of the O-induced D_2O desorption. An incident O atom abstract a D adatom to form a hot OD* molecule which then abstracts a nearby D atom to form a D_2O molecule.

5.5 Conclusion

I studied atomic O-induced D abstraction from monodeuteride and monodeuteride/dideuteride surfaces using a continuous as well as a pulsed O-beam. Both D_2 and D_2O molecules were desorbed from the surfaces. The Si dideuterides were committed to the D_2 and D_2O desorption. From the pulsed O-beam experiments, both of the D_2 and D_2O desorptions were found to be prompt in nature. The evaluated reaction order in the D_2 desorption from the O-free surfaces followed a second-order rate law on the monodeuteride surface and nearly fourth-order rate law on the monodeuteride/dideuteride surface. On the other hand, the O-induced D_2O desorption reaction was governed by a nearly second-order rate law with respect to initial D coverage (θ°_{D}). Based on these results, atomistic mechanisms of the O-induced reactions on the D covered Si(100) surface were proposed. The formation of water molecules from O and H atoms on surfaces may be an alternative relevance to the space chemistry, since interstellar hydrogen molecules, which nucleate to bear new stars, are anticipated to be produced on water ice surfaces over fine dust grains.[13] The problem is that how and where H_2O molecules are formed from O and H atoms in the space is still obscure.[13,14] On the basis of the present study, we anticipate that H_2O molecules are formed on the surfaces of fine silicate dust grains through the reaction $O + H_{ad} \rightarrow H_2O$.

References

1. S. Shimokawa, F. Khanom, T. Fujimoto, S. Inanaga, A. Namiki, T. Ando, Appl. Surf. Sci. 167 (2000) 94
2. F. Rahman, F. Khanom, S. Inanaga, H. Tsurumaki, A. Namiki, Appl. Surf. Sci. 220 (2003) 1
3. A. Chatterjee, T. Iwasaki, T. Ebina, M. Kubo, A. Myamoto, J. Phys. Chem. B 102 (1998) 9215.
4. K. Kato, H. Kajiyama, S. Heike, T. Hashizume, T. Uda, Phys. Rev. Lett. 86 (2001) 2842.
5. J.A. Schaefer, D. Frankel, F. Stucki, W. Go¨ pel, G.J. Lapeyre, Surf. Sci. 139 (1984) L209.
6. Y. Sugita, S. Watanabe, Jpn. J. Appl. Phys. 37 (1998) 3272.
7. H. Tsurumaki, K. Iwamura, T. Karato, S. Inanaga, A. Namiki, Phys. Rev. B 67 (2003) 155316.
8. F. Rahman, H. Kuroda, T. Kiyonaga, F. Khanom, H. Tsurumaki, S. Inanaga, A. Namiki, J. Chem. Phys. 121 (2004) 3221.
9. S. Inanaga, H. Goto, A. Takeo, F. Rahman, F. Khanom, H. Tsurumaki, A. Namiki, Surf. Sci. 596 (2005) 82.
10. E. Hayakawa, F. Khanom, T. Yoshifuku, S. Shimokawa, A. Namiki and T. Ando, Phys. Rev. B. 65 (2001) 033405.
11. H. H. Kan, R. B. Shumbera and J. F. Weaver, J. Chem. Phys. 126 (2007) 134704.
12. H. Ikeda, K. Hotta, T. Yamada, S. Zaima, H. Iwano, Y. Yasuda, J. Appl. Phys. 77 (1995) 5125.
13. D. A. Williams and E. Herbst, Surf. Sci. 500 (2002) 823.
14. J. M. Greenberg, Surf. Sci. 500 (2002) 793